Soft Matter

Self-healing Hydrogels Containing Reversible Oxime Crosslinks

Journal:	*Soft Matter*
Manuscript ID:	SM-ART-04-2015-000865.R1
Article Type:	Paper
Date Submitted by the Author:	22-Jun-2015
Complete List of Authors:	Mukherjee, Soma; University of Florida, Department of Chemistry Hill, Megan; University of Florida, Chemistry Sumerlin, Brent; University of Florida, Department of Chemistry;

Journal Name

RSCPublishing

ARTICLE

Self-healing Hydrogels Containing Reversible Oxime Crosslinks

Cite this: DOI: 10.1039/x0xx00000x

Soma Mukherjee,[a] Megan R. Hill[a] and Brent S. Sumerlin*[a]

Received 00th January 2012,
Accepted 00th January 2012

DOI: 10.1039/x0xx00000x

www.rsc.org/

Self-healing oxime-functional hydrogels have been developed that undergo a reversible gel-to-sol transition *via* oxime exchange under acidic conditions. Keto-functional copolymers were prepared by conventional radical polymerization of *N,N*-dimethylacrylamide (DMA) and diacetone acrylamide (DAA). The resulting water soluble copolymers (P(DMA–*stat*–DAA)) were chemically crosslinked with difunctional alkoxyamines to obtain hydrogels *via* oxime formation. Gel-to-sol transitions were induced by the addition of excess monofunctional alkoxyamines to promote competitive oxime exchange under acidic conditions at 25 °C. The hydrogel could autonomously heal after it was damaged due to the dynamic nature of the oxime crosslinks. In addition to their chemo-responsive behavior, the P(DMA–*stat*–DAA) copolymers exhibit cloud points which vary with the DAA content in the copolymers. This thermo-responsive behavior of the P(DMA–*stat*–DAA) was utilized to form physical hydrogels above their cloud point. Therefore, these materials can either form dynamic-covalent or physically-crosslinked gels, both of which demonstrate reversible gelation behavior.

Introduction

Polymers have become one of the most essential components in microelectronics, surface coatings, lightweight aerospace materials, drug-delivery systems, regenerative medicine, dental fillings, prosthetic limbs, and artificial heart valves.[1] However, polymeric engineering materials used for such purposes often suffer mechanical failure leading to limited life span because of the continuous exposure to chemical and mechanical stresses.[1,2] To extend the life span of polymeric materials, research in the area of self-mendable or self-healing polymers is growing rapidly. Self-healing is one of the most fascinating features of biological systems, such as skin, bones, and muscle tissues, and this phenomena has inspired the scientific community for decades to design synthetic auto-repairable materials.[3] The ability of self-healing polymers to reorganize themselves at a molecular level after a mechanical damage renders them very suitable for sensing applications, designing shape-memory materials, and increasing the life-time of surface coatings.[4]

The process of healing cracks in natural systems often involves an energy dissipation mechanism, due to the presence of sacrificial bonds that can break and reform dynamically before or while the failure occurs.[5] Several covalent (*e.g.*, Diels-Alder linkages, hydrazone bonds, alkoxyamines, and disulfide linkages)[6,7] and non-covalent interactions (*e.g.,* hydrogen bonding, π-π stacking, ionic interactions, and metal-ligand coordination)[8,9] have been employed to prepare self-healing polymers. However, the use of reversible-covalent or dynamic-covalent interactions to prepare such materials remains a particularly interesting possibility for creating robust materials that are covalently crosslinked, while maintaining the dynamic nature that allows healing by bond reorganization.[10] Moreover, incorporation of labile covalent bonds into densely crosslinked macromolecules allows not only the tailoring of their mechanical properties but also the tuning of their macroscopic response when exposed to a stimulus.

Among the various branched/crosslinked polymeric architectures, hydrogels have been studied extensively for diverse biomedical applications.[6,9,11,12-14] Hydrogels are three dimensional crosslinked polymeric networks swollen in large amounts of water that have many of the characteristics of cellular environments, such as their high water content, the diffusivity of small molecules in the hydrogel matrix, and comparable elasticity and mechanical properties that are often similar to those of soft tissue.[15,16] These materials are often considered as prime candidates for biosensors, delivery vehicles for drugs and biomolecules, and carriers or matrices for cells in tissue engineering. Traditionally, hydrogels have been synthesized by non-covalent and covalent crosslinking in attempts to mimic biological environments. However, the majority of these hydrogels lack the dynamic properties necessary for many complex tissue processes. Recent attempts to introduce dynamic complexity into hydrogels, more specifically, responsiveness to biological stimuli or sol-to-gel transition behavior, have begun to address some of the very fundamental questions about how synthetic hydrogels function in

cellular environments.[15] For example, introduction of hydrolytically degradable components in PEG- and hyaluronic-based hydrogels containing encapsulated mesenchymal stem cells for cartilage tissue engineering can lead to more uniform tissue distribution and cellular organization due to the improved distribution of chondroitin sulfate, an extra cellular matrix molecule in the cartilage.[17] Recently Jiang *et al.* demonstrated a liquid lens system consisting of a pH- and temperature-responsive hydrogel which could actuate adjustments to the shape and, accordingly, the focal length and autonomous focus of a liquid droplet contained in the hydrogel by sensing the change in pH/temperature of the medium.[18] Hydrogels have also been designed to sense other environmental changes, such as light intensity,[19] electric signals,[20] redox potentials,[14,21] and variations in glucose concentration.[22]

Incorporation of reversible bonds in hydrogels allows post-synthetic tailoring of network properties, such as crosslink density, swelling, and mechanical strength.[23] A variety of reversible linkages have been utilized in the past to prepare stimuli-responsive hydrogels having self-healing capabilities. For example, Chen *et al.* investigated the reversible sol-to-gel transition and self-healing properties of organo-/hydrogels having acyl hydrazone bonds, and reported the gelation kinetics and mechanical properties of acyl hydrazone-containing organogels.[6,12,24] In another report Anseth *et al* have shown that the temperature and pH of the reaction medium influenced the reaction rate constant of acyl hydrazone formation, and the reverse reaction rate constant affected the stress relaxation characteristics of the acyl hydrazone-containing hydrogel.[25] Fulton and coworkers, demonstrated an interesting reversible transformation from acyl hydrazone-containing single chain nanoparticles (SCNP) to chemically crosslinked hydrogels, facilitated by intermolecular reorganization of the collapsed polymer chains when the SCNPs were heated above their lower critical solution temperature.[26] Diels-Alder chemistry is another widely used method to design degradable hydrogels, and recently both Bowman *et al*. and Goepferich *et al.* demonstrated that poly(ethylene glycol) based hydrogels containing furan-maleimide Diels-Alder linkages could degrade at human body temperatures by the retro Diels-Alder mechanism.[27] Several other reversible bonds, such as imines,[13] disulfides,[28] boronate esters,[29,30] and thermoreversible alkoxyamines[31] have been used to construct dynamic-covalent hydrogels, however, the reversibility of oxime-containing hydrogels has yet to be explored.

Oxime ligation has proven particularly promising for bioconjugation, due to the high reaction efficiency, ambient reaction conditions, benign side product (*i.e.*, water), and most importantly, the superior hydrolytic stability of oxime bonds.[32,33,34] Maynard *et al.* incorporated oxime bonds into hydrogels that can encapsulate stem cells and support cell adhesion.[35] Oxime ligation was also utilized by Becker *et al.* to prepare poly(ethylene glycol)-based hydrogels for three-dimensional patterning of peptides onto a hydrogel matrix by photoinitiated thiol-ene chemistry.[36] However, there are limited examples of exploiting the controlled exchange behavior of oxime linkages, even in small molecule chemistry,[34,37] and it is only recently that our group has demonstrated the synthesis and characterization of oxime-containing core-crosslinked star polymers that can degrade by competitive oxime exchange within the core.[38]

Inspired by our recent success with core-crosslinked star polymers,[38,39] we reasoned that the controlled exchange behavior of oxime bonds could be tuned to obtain self-repairable hydrogels having reversible sol-to-gel transition capabilities under suitable conditions. The covalent nature of the oxime bond is expected to contribute to the mechanical integrity of the hydrogel matrix, while the reversibility of oxime bonds will allow the components to reshuffle at the molecular level when under stress to effect healing. Herein, we describe the synthesis of novel hydrogels that contain oxime crosslinks and are capable of autonomous healing due to their dynamic nature. The reversible sol-to-gel transition was induced in the presence of excess monofunctional alkoxyamine and an acid catalyst.

EXPERIMENTAL SECTION

Materials. *N,N*–Dimethylacrylamide (DMA, Fluka, 98%) was passed through a small column of basic alumina to remove inhibitor prior to polymerization. Diacetone acrylamide (DAA, Sigma Aldrich, 99%) was recrystallized from hexane. 2,2′–Azobisisobutyronitrile (AIBN, Sigma Aldrich, 98%) was recrystallized from ethanol. *O*–(Tetrahydro–2H–pyran–2–yl)hydroxylamine (Sigma Aldrich, 96%), *O*–allyl hydroxylamine hydrochloride (Fluka , ≥98.0%), *O,O′*–1,3–propanediylbishydroxylamine dihydrochloride (Sigma Aldrich, >99%), cresol red sodium salt (Alfa Aesar), trifluoroacetic acid (TFA, EMD Millipore, 99.5%), triethyl amine (TEA, Fisher Chemical, 99%), 1,3,5–trioxane (Acros Organics, 99.5%), *N,N*–dimethylformamide (DMF, EMD, 99.9%), *N,N*–dimethyl acetamide (DMAc, Sigma Aldrich, 99.9%), tetrahydrofuran (THF, EMD, 99.5%), dichloromethane (DCM, BDH, 99.5%), 1,4–dioxane (Fisher Chemicals, 99%), phosphate buffered saline (PBS, pH 7, Sigma Aldrich), methanol (Mallinckrodt, 99.8%), ethyl acetate (Fisher chemicals, 99.9%), hexane (BDH, 98.5%,), dimethylsulfoxide–d_6 (DMSO-d_6, Cambridge Isotope, 99.9% D), and $CDCl_3$ (Cambridge Isotope, 99% D) were used as received.

Instrument and analysis. Molecular weights and molecular weight dispersities were determined by size exclusion chromatography (SEC). SEC was performed with 0.05 M LiCl in DMAc at 55 °C and a flow rate of 1.0 mL/min (Agilent isocratic pump, degasser, and autosampler, columns: PLgel 5 μm guard + two ViscoGel I-series G3078 mixed bed columns: molecular weight range 0–20 × 10^3 and 0–100 × 10^4 g/mol). Detection consisted of a Wyatt Optilab T-rEX refractive index detector operating at 658 nm and a Wyatt miniDAWN TREOS light scattering detector operating at 659 nm. Absolute molecular weights and molecular weight dispersities were calculated using the Wyatt ASTRA software. Dynamic light scattering (DLS) was conducted at 173° with a Malvern Zetasizer Nano–ZS equipped with a 4 mW, 633 nm He–Ne laser and an Avalanche photodiode detector. UV-Vis spectroscopic measurements were conducted with a Varian Cary 500 Scanning UV-Vis-NIR spectrophotometer. Proton NMR spectra were recorded using Inova spectrometers operating at 500 MHz. Chemical shifts are reported in parts per million (ppm) downfield relative to tetramethylsilane (TMS, 0.0 ppm). The lyophilized hydrogel samples were examined and digital micrographs acquired by field-emission scanning electron microscope (S-4000, Hitachi High Technologies America, Inc. Clarksburg, MD USA). The hydrogel samples were mounted on carbon adhesive tabs on aluminum specimen mounts. Samples for SEM were rendered conductive with an Au/Pd sputter coater (DeskV, Denton Vacuum, Moorestown, NJ USA). The mechanical properties of the hydrogels were determined by rheological experiments on a TA Instruments ARES LS1 rheometer using 25 and 50 mm cone and plate geometries for gelation kinetics and parallel plate geometries for pre-formed gels. A solvent trap was used to minimize solvent loss during long experiments.

Conventional radical polymerization of DMA and DAA (P(DMA–*stat*–DAA), P2). A typical procedure for the synthesis of P(DMA–*stat*–DAA) was as follows.

DMA (14.0 g, 0.194 mol), DAA (3.64 g, 0.0215 mol), AIBN (0.0214 g, 0.129 mmol), *s*-trioxane (0.193 g, 2.16 mmol), and 1,4–dioxane (25 mL) were sealed in a 100 mL round bottom flask with a rubber septum and purged with nitrogen for 40 min. The reaction flask was then placed on a preheated silicon oil bath at 60 °C. Samples were removed periodically using a degassed syringe to determine monomer conversion by ^{1}H NMR spectroscopy. The polymerization was quenched after 52 min at 48% conversion of DMA by removing the round bottom flask from the oil bath and opening it to expose its contents to atmospheric oxygen. The reaction solution was dialyzed in DI water through a regenerated cellulose dialysis tubing having a molecular weight cut-off (MWCO) = 3.5 kg/mol, and the product was isolated by lyophilization resulting in poly(*N,N*–dimethylacrylamide-*stat*-diacetone acrylamide) (P($DMA_{0.68}$–*stat*–$DAA_{0.32}$), *(i.e.*, a copolymer with mole fractions of DMA and DAA equal to 0.68 and 0.32, respectively) **P2**) ($M_{n,\ SEC\text{-}MALS}$ = 309 kg/mol and M_w/M_n = 1.33). A similar procedure was followed to prepare P($DMA_{0.72}$–*stat*–$DAA_{0.28}$) (**P1**), P($DMA_{0.60}$–*stat*–$DAA_{0.40}$) (**P3**), and P($DMA_{0.52}$–*stat*–$DAA_{0.48}$) (**P4**).

Preparation of organogel with P(DMA–*stat*–DAA). To study gel formation in an organic medium such as methanol, P($DMA_{0.52}$–*stat*–$DAA_{0.48}$) (**P4,** 0.050 g, 0.18 mmol) was dissolved in methanol (0.25 mL) in a 4 mL vial. *O,O′*–1,3–Propanediylbishydroxylamine dihydrochloride (0.055 g, 0.31 mmol) was added to a mixture of methanol (1 mL) and TEA (0.086 mL, 0.62 mmol) under stirring. An aliquot (0.214 mL) of the resulting solution was added to the polymer solution, and the reaction vial was kept on a mechanical shaker at 25 °C until the solution gelled and stopped flowing. The gel formation was confirmed by vial inversion.

Organogels with other polymers at different polymer concentrations (0.1 g/mL and 0.05 g/mL) and different stoichiometries (*i.e.*, [ketone]:[alkoxyamine] = 1:1) were prepared in a manner similar to that described above.

Preparation of hydrogel with P(DMA–*stat*–DAA). To study the hydrogel formation, P($DMA_{0.52}$–*stat*–$DAA_{0.48}$), **P4** (0.050 g, 0.18 mmol) was dissolved in PBS (pH 7, 0.25 mL) in a 4 mL vial. *O,O′*–1,3–Propanediylbishydroxylamine dihydrochloride (0.050 g, 0.28 mmol) was dissolved in PBS (1 mL), and an aliquot (0.21 mL) of the resulting solution was added to the polymer solution. The reaction vial was kept on a mechanical shaker at 25 °C until the solution turned into a gel and stopped flowing. Gel formation was confirmed by vial inversion and characterized by rheometry.

Hydrogels with other polymers at different polymer concentrations (*e.g.,* 0.1 g/mL and 0.05 g/mL) and different stoichiometries (*i.e.*, [ketone]:[alkoxyamine] = 1:1) were prepared and characterized in a manner similar to that described above.

Determination of mass swelling ratio of hydrogels. The hydrogels used for determining swelling ratio were prepared in a manner similar to that described above and were dialyzed against deionized water. The increase in hydrogel weight was monitored until there was no further change in weight. The hydrogels were lyophilized to obtain the dry gel. The experiment was repeated with 3-4 hydrogel samples. Mass swelling ratio was determined by

Mass swelling ratio = (Mass of swollen gel - Mass of dry gel)/Mass of dry gel.

Determination of the cloud point of P(DMA–*stat*–DAA) by turbidity. P($DMA_{0.6}$–*stat*–$DAA_{0.4}$), **P3** (0.5 mg) was dissolved in deionized water (1 mL), and the resulting solution was transferred into a glass cuvette for turbidity studies using a UV-Vis spectrophotometer. The change in transmittance values with increasing temperature was recorded to obtain the cloud point, defined here as the temperature corresponding to 50% reduction of transmission at 500 nm of the polymer.

Preparation of thermoresponsive hydrogel with P(DMA–*stat*–DAA). P($DMA_{0.6}$–*stat*–$DAA_{0.4}$), **P3** (0.10 g, 0.31 mmol) was dissolved in PBS (pH 7, 0.5 mL), and the solution was heated above the cloud point of the polymer (*i.e.*, 61 °C) to induce gelation. Gel formation was confirmed by the vial inversion and oscillatory rheological measurements. Thermoresponsive hydrogel with P($DMA_{0.52}$–*stat*–$DAA_{0.48}$) was prepared in a similar manner.

Hydrogel-to-sol transition. P($DMA_{0.68}$–*stat*–$DAA_{0.32}$), **P2** (0.10 g, 0.26 mmol) was dissolved in PBS (pH 7, 1 mL), and the resulting solution (0.3 mL) was transferred to a 4 mL vial. *O,O′*–1,3–Propanediylbishydroxylamine dihydrochloride (0.050 g, 0.28 mmol) was dissolved in PBS (1 mL), and the resulting solution (0.098 mL) was added to the polymer solution in the vial. The reaction solution was kept on a mechanical shaker for four days to mature the resulting hydrogel. *O*–(Tetrahydro–2*H*–pyran–2–yl)hydroxylamine (0.20 g, 1.7 mmol) was dissolved in PBS (pH 7), the resulting solution (0.16 mL) and TFA (10 μL) were added to the hydrogel, and the reaction vial was placed on a mechanical shaker. The change in viscosity of the reaction mixture was observed visually at different time intervals to monitor the gel-to-sol transition. The other hydrogels were investigated in a similar manner.

Rheological investigation of gelation kinetics and mechanical properties. Two different geometries (either 25 or 50 mm cone and plate) were used to study the hydrogel formation kinetics using a TA ARES LS1 rheometer. The viscoelastic region for each hydrogel was determined by a dynamic strain sweep experiment with a preformed hydrogel at a frequency of 10 rad/s and 25 °C. For a typical dynamic time sweep experiment P($DMA_{0.68}$–*stat*–$DAA_{0.32}$) (0.020 g, 0.053 mmol) was dissolved in PBS (pH 7, 0.1 mL), and the solution was transferred onto the 25 mm plate. *O,O′*–1,3–Propanediylbishydroxylamine dihydrochloride (0.050 g, 0.28 mmol) was dissolved in PBS (1 mL) and an aliquot (0.095 mL) of the resulting solution was added to the polymer solution on the plate before mixing homogeneously for 43-45 s. A solvent trap was used during the test to prevent solvent loss. The time sweep experiment was carried out at a frequency of 10 rad/s, 1% strain at 25 °C to obtain the crossover point of the storage and loss modulus values (G' and G'', respectively). A frequency sweep test was conducted with a preformed gel at 25 °C and a constant strain (1% or 2% strain). All the experiments were repeated at least 3 times.

A similar procedure was followed to characterize the other hydrogels.

Rheological studies of thermoresponsive hydrogels. P($DMA_{0.6}$–*stat*–$DAA_{0.4}$) (**P3**, 0.10 g, 0.31 mmol) was dissolved in PBS (pH 7, 0.5 mL), and the resulting solution (0.2 mL) was transferred to the 25 mm plate. A dynamic temperature-step test was carried out at a frequency of 10 rad/s, 1% strain, from 25 to 65 °C in 3 consecutive cycles. A dynamic temperature-step experiment with P($DMA_{0.52}$–*stat*–$DAA_{0.48}$) was carried out in a similar manner.

Self-healing study of hydrogels. Self-healing was carried out with preformed hydrogels prepared at either [P($DMA_{0.68}$–*stat*–$DAA_{0.32}$)] = 0.05 g/mL and [ketone]:[alkoxyamine] = 1.5:1 or [P($DMA_{0.68}$–*stat*–$DAA_{0.32}$)] = 0.2 g/mL and [ketone]:[alkoxyamine] = 1:1. P($DMA_{0.68}$–*stat*–$DAA_{0.32}$) (0.20 g, 0.53 mmol) was dissolved in PBS (pH 7, 1 mL), and two portions of the resulting solution (0.18 mL each) were transferred into two silicone molds on a glass plate. A

solution of cresol red (0.015 mL, 0.050 g/mL) was added to one of the molds containing polymer solution and mixed well. *O,O'*–1,3–Propanediylbishydroxylamine dihydrochloride (0.050 g, 0.28 mmol) was dissolved in PBS (1 mL), and two portions (0.17 mL each) of the resulting solution were added to both polymer solutions in the mold and mixed well. The molds were kept in a closed Petri dish saturated with moisture and allowed to mature for four days before study. The hydrogels were cut in half, and the cut surface of one half of the clear hydrogel was kept in contact with one half of the colored hydrogel. Healing was confirmed by stretching the healed hydrogel with tweezers from both sides of the cut after 2 h and also by the ability of the healed hydrogel to hold its structure when suspended under gravity for months. The experiment was repeated three more times by cutting the healed sample along the same line of the previous cut and also in a perpendicular direction. Each time the healed hydrogel was matured for 24 h before being cut again.

Self-recovery study using rheometer. A preformed hydrogel prepared with P($DMA_{0.68}$–*stat*–$DAA_{0.32}$) (**P2,** 0.2 g/mL) and 1 equivalence of the dialkoxyamine crosslinker (0.05 g/mL) in a manner similar to that described above was used for the strain sweep test (0.1-1000% strain). The hydrogel was matured for 2 h before intentionally damaging it during a strain sweep test. The hydrogel was broken with high strain, and the recovery of the hydrogel was observed with a time sweep at 1% strain, 10 rad/s frequency at 25 °C using a 25 mm CP geometry. A similar procedure was adopted for the hydrogel prepared with P($DMA_{0.68}$–*stat*–$DAA_{0.32}$) (**P2**, 0.05 g/mL) at [ketone]:[alkoxyamine] = 1.5:1 using a 50 mm CP geometry. The hydrogel was matured for 3 h before beginning the strain sweep experiment.

RESULTS AND DISCUSSION

We were interested in creating crosslinked polymeric materials by incorporating reversible linkages that were hydrolytically stable under most conditions in aqueous media but were susceptible to dynamic exchange when triggered by a change in pH or the addition of specific small molecules. This dynamic behavior is the result of linkages that can be reversibly disassembled and reformed under thermodynamic equilibrium.[40] Incorporation of the dynamic or reversible oxime bonds in the hydrogels was expected to not only induce reversible sol-to-gel transition by competitive exchange with excess aminooxy compounds, but also to enable the system to heal autonomously after damage. Diacetone acrylamide (DAA) and *N,N*–dimethylacrylamide (DMA) were copolymerized by conventional radical polymerization to obtain keto-functional hydrophilic copolymers with varying DAA content (Scheme 1). The resulting ketone-containing copolymers were crosslinked with a difunctional alkoxyamine in aqueous media to result in hydrogels containing the condensation product of the pendent ketone and alkoxyamine (*i.e.,* ketoximes). The reversible nature of the hydrogels was first demonstrated by the gel-to-sol transition in the presence of excess monofunctional alkoxyamine. As detailed below, the hydrogels were able to self-repair by oxime exchange after damage occurred. The mechanical properties of the hydrogels were studied by rheometry.

Synthesis of keto-functional copolymers and formation of supramolecular hydrogel. DAA was chosen as a comonomer due to its keto functional group, which could be modified with an alkoxyamine compound by the highly efficient oxime formation reaction. DAA was copolymerized with DMA by conventional radical polymerization to obtain P(DMA_m–*stat*–DAA_n) with the mole fraction of DAA (*m*) content varying from 0.28 to 0.48 (Table 1). The number average molecular weight (M_n) of the polymers was determined by SEC. The amount of DAA incorporated in the copolymer was obtained by ^{1}H NMR spectroscopy by comparing the area of the methyl protons in the DMA unit (–N–(C$\underline{H}_3$)$_2$, δ = 2.90 ppm) and the area of the methyl protons (–(C=O)–C$\underline{H}_3$, δ = 2.04 ppm) in the DAA unit in the P(DMA–*stat*–DAA) copolymers (Fig. S1).

Scheme 1. Synthesis of P(DMA_m-*stat*-DAA_n)

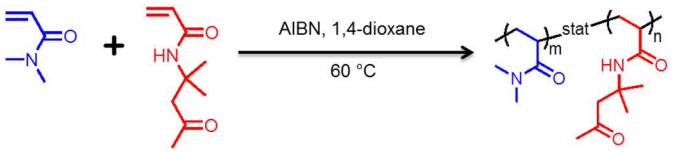

Table 1 Copolymers with *N,N*–Dimethylacrylamide (DMA) and Diacetone Acrylamide (DAA)

Entry	Polymer	$M_{n,SEC}$[a] (kg/mol)	$M_{w,SEC}$[a] (kg/mol)	M_w/M_n[a]	DAA mole %[b]
P1	P($DMA_{0.72}$–*stat*–$DAA_{0.28}$)	250	370	1.48	28
P2	P($DMA_{0.68}$–*stat*–$DAA_{0.32}$)	309	412	1.33	32
P3	P($DMA_{0.60}$–*stat*–$DAA_{0.40}$)	271	371	1.37	40
P4	P($DMA_{0.52}$–*stat*–$DAA_{0.48}$)	277	395	1.42	48

[a]Determined by SEC with multiangle light scattering detection. [b]Calculated from ^{1}H NMR spectroscopy.

Recently Cai *et al.* reported DAA–containing copolymers having tunable aqueous solubility in response to temperature.[41] We were interested in investigating whether the DAA within our P(DMA–*stat*–DAA) copolymers could impart composition-dependent thermoresponsive behavior to our hydrogels.[42] Interestingly, the copolymers P($DMA_{0.52}$–*stat*–$DAA_{0.48}$) and P($DMA_{0.6}$–*stat*–$DAA_{0.4}$) exhibited cloud points of 34 and 61 °C, respectively, for solutions of 0.5 mg/mL (Fig. S2). However, copolymers with lower contents of DAA did not demonstrate thermoresponsive behavior, with solutions (0.5 mg/mL) of P($DMA_{0.68}$–*stat*–$DAA_{0.32}$) and P($DMA_{0.72}$–*stat*–$DAA_{0.28}$) remaining homogeneous up to 70 °C. When the aqueous solutions of P($DMA_{0.6}$–*stat*–$DAA_{0.4}$) and P($DMA_{0.52}$–*stat*–$DAA_{0.48}$) (0.2 g/mL in PBS, pH 7) were heated, the copolymers demonstrated temperature-responsive solubility. Interestingly, at this relatively high concentration, the solutions became opaque as the polymer chains collapsed and the solutions gelled, as confirmed by vial inversion (Fig. 1 and Fig. S3). To understand the supramolecular gelation process further, a rheological temperature-step experiment was carried out.

The polymer solution was heated and cooled in cycles, and the change in modulus was monitored over time. A gradual increase in G' was observed as the polymer solution was heated to close to its cloud point, during which G' eventually exceeded G''. The reversible nature of this phenomenon was demonstrated by carrying out the temperature-step experiment over several cycles (Fig. 1 and Fig. S3). Notably, the initial G' of the second and third heating cycles were greater than the G'', and the crossover temperature varied during the different cycles. This behaviour is possibly due to the presence of residual physical aggregation and chain entanglement that persists after cooling below the cloud point of the polymer. The kinetics of demixing and remixing and the elastic properties of physical hydrogels can be complicated by a variety of factors, including heating rate and the onset of phase separation and sedimentation above the cloud point.[43] Even though a thorough and more detailed investigation is required to interpret the nature of the supramolecular gelation process, the current result nicely shows that the DAA polymers could be well utilized to form physically crosslinked hydrogels.

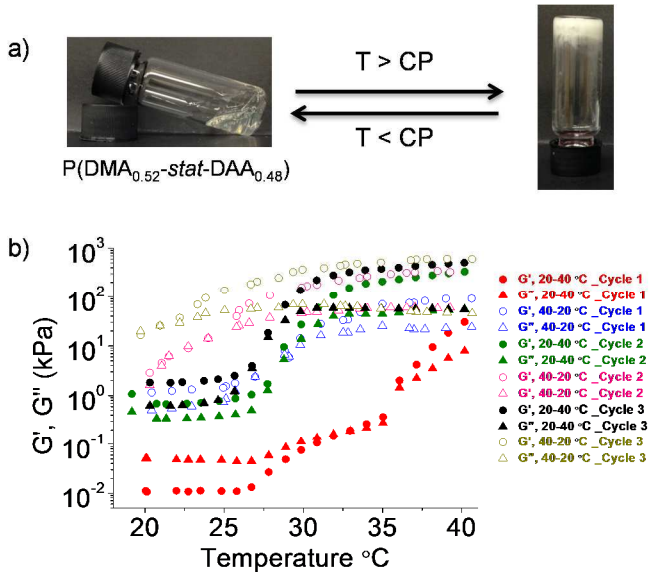

Fig. 1 Reversible sol-to-gel transitions of P($DMA_{0.52}$-*stat*-$DAA_{0.48}$) (a) by vial inversion and (b) by temperature step rheology experiments at 10 rad/s and 1% strain. Upon heating, the thermoresponsive nature of these copolymers led to reversible physical gelation.

Hydrogels from P(DMA_m–*stat*–DAA_n) and difunctional alkoxyamines. Given the high efficiency of oxime formation in aqueous media, as demonstrated previously by our group and others,[33,38,44] we believed the reaction of polymer-bound ketones and multifunctional alkoxyamines could be a viable means to prepare densely-crosslinked polymeric networks, such as hydrogels or organogels. The minimum concentration of P(DMA_m–*stat*–DAA_n) and the [ketone]:[alkoxyamine] ratio required for gel formation were determined to be 0.05 g/mL and 1.5:1, respectively, in aqueous and organic (methanol) media. Considering the utility of hydrogels for many biological applications, we decided to focus on gel formation in aqueous media. Hydrogel formation was triggered by mixing the polymer solution in PBS (pH 7) with a solution of *O,O'*–1,3–propanediylbishydroxylamine dihydrochloride in PBS (pH 7) at 25 °C (Fig. 2). To obtain more insight into the effect of polymer concentration and stoichiometry on the hydrogel formation kinetics, we carried out rheology experiments employing three different polymer concentrations (*i.e.,* 0.05, 0.1, and 0.2 g/mL) and two different stoichiometries (*i.e.,* [ketone]:[alkoxyamine] = 1:1 and 1.5:1) (Fig. 2). Gel formation was also confirmed more qualitatively by the vial inversion method (Fig. 2).

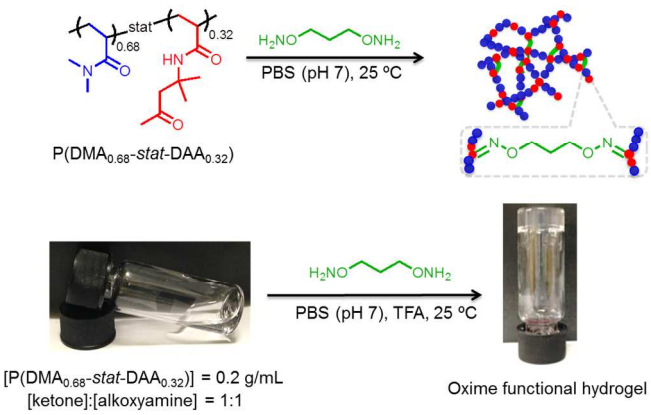

Fig. 2 Hydrogel formation with P($DMA_{0.68}$–*stat*–$DAA_{0.32}$) at polymer concentrations 0.2 g/mL and [ketone]:[alkoxyamine] = 1:1 at 25 °C.

For rheological experiments, a dynamic strain sweep was carried out to determine the linear viscoelastic region of the gel. A dynamic time sweep was conducted to observe the elastic modulus (G') and viscous modulus (G'') for hydrogels formed at different polymer concentrations and stoichiometries. For example, solutions of P($DMA_{0.68}$–*stat*–$DAA_{0.32}$) in PBS were mixed with solutions of the difunctional alkoxyamine crosslinker ([ketone]:[alkoxyamine] = 1:1 or 1.5:1), and the rheological measurements were started after a brief period of mixing. In all cases, G' increased with time and eventually exceeded G'', indicating the approximate onset of gelation. The value of crossover time for the hydrogel formation reaction decreased with increasing polymer concentration due to the enhanced rate of the crosslinking reaction (Fig. 3). For example, the value of crossover time was ~102 s for the hydrogel prepared with P($DMA_{0.68}$–*stat*–$DAA_{0.32}$) at 0.1 g/mL and [ketone]:[alkoxyamine] = 1.5:1, while the hydrogel formed at a concentration of 0.2 g/mL copolymer with a similar stoichiometry led to a crossover time of ~38 s. However, no significant change in G' was noticed when the crosslinker equivalence alone was increased (Fig. 3), suggesting the concentration of crosslinker had less impact on gelation kinetics than the concentration of copolymer. The gelation reactions were observed until the G′ of the hydrogels reached a near constant value (Fig. S4).

The ketone content in the copolymer available for crosslinking with the dialkoxyamine had a significant impact on the gelation kinetics and hydrogel properties. Gelation was significantly faster with increasing DAA content in the parent copolymer. In fact, the copolymer with the highest DAA content (P($DMA_{0.52}$–*stat*–$DAA_{0.48}$)) gelled immediately upon addition of the difunctional alkoxyamine, even before the time sweep experiment could be started. Ketone content also played a key role in determining hydrogel strength. For example, under identical conditions (0.2 g/mL copolymer, [ketone]:[alkoxyamine] = 1:1, 25 min), the equilibrium storage modulus of the hydrogels observed during the dynamic time sweep experiment were 4.1, 13, and 75 kPa for the hydrogels prepared from copolymers containing 32, 40, and 48% DAA, respectively. This result is consistent with increased gel strength with increasing crosslink density. In all cases, the G' values of the

hydrogels did not change significantly with frequency, suggesting tthe frequency scale probe (>0.1 rad/s) was faster than the rate needed for the oxime links to rearrange themselves (Fig. 4b).[6] The hydrogels were also imaged by SEM to observe the effect of ketone content on pore structure. As expected, higher DAA content in the copolymers (*i.e.*, increased crosslink density in the gels) resulted in smaller pore sizes (Fig. 5) and reduced swelling ratios (Fig. S5).

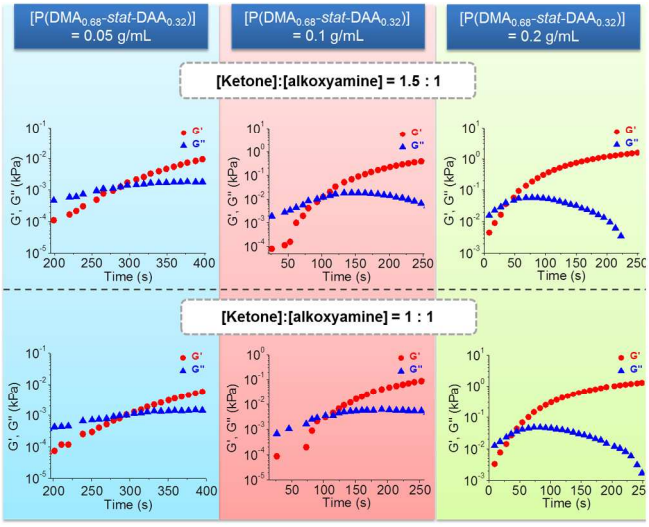

Fig. 3 Dynamic time sweep experiments with P(DMA$_{0.68}$-*stat*-DAA$_{0.32}$) at different concentrations (*i.e.*, 0.05 g/mL, 0.1 g/mL, and 0.2 g/mL) and different [ketone]:[alkoxyamine] ratios (*i.e.*, 1.5:1 and 1:1) at 1% strain, 10 rad/s, and 25 °C. These results indicate gelation was faster with increasing polymer concentration, while the ratio of [ketone]:[alkoxyamine] groups had less of an effect.

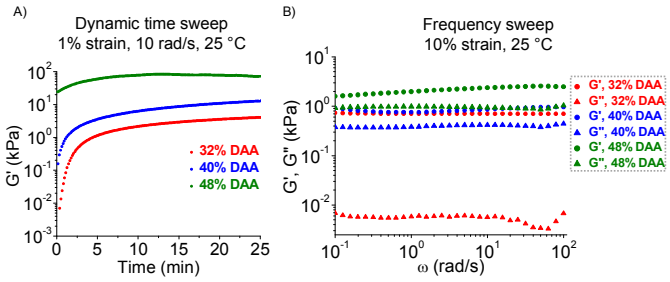

Fig. 4 Rheological experiments of P(DMA–*stat*–DAA) copolymers with varying DAA content. (a) Evolution of storage modulus (G') with time in a dynamic time sweep experiment ([copolymer] = 0.2 g/mL, [ketone]:[alkoxyamine] = 1:1, 10 rad/s, 1% strain, and 25 °C). (b) Evolution of hydrogel storage and loss moduli (G', G'') in a frequency sweep experiment ([copolymer] = 0.2 g/mL, [ketone]:[alkoxyamine] = 1:1, 2% strain and 25 °C).

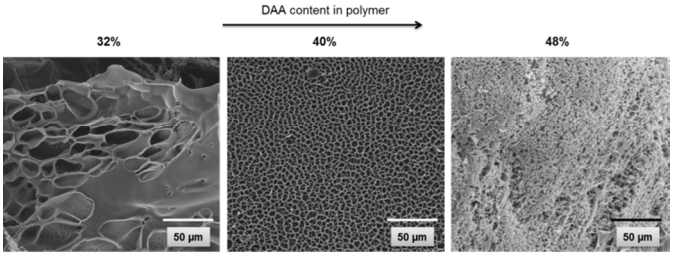

Fig. 5 SEM images of hydrogels prepared with 32, 40, and 48% DAA-containing P(DMA$_m$–*stat*–DAA$_n$) copolymers after they are dialyzed against deionised water and lyophilized. Increasing DAA content led to increased crosslink density and decreased pore size.

Gel-to-sol transition. While oxime-functional hydrogels have been utilized for pattern formation and peptide encapsulation,[36] stem cell encapsulation,[35] and as an injectable delivery systems,[45] their reversible gel-to-sol transition and self-mending ability has remained largely unexplored. Oxime-containing polymers can be rendered dynamic, as we recently reported for the reversible disassembly of core-crosslinked star polymers containing oxime-functional cores.[38] We envisioned that incorporation of such reversible bonds in a hydrogel matrix would allow the gels to undergo a gel-to-sol transition upon cleavage of the crosslinks during addition of excess monofunctional alkoxyamine that would compete for binding with the polymer-bound ketones. Indeed, addition of 20 equiv *O*–(tetrahydro–2*H*–pyran–2–yl)hydroxylamine along with catalytic TFA led to dissociation of hydrogels prepared with P(DMA$_{0.68}$–*stat*–DAA$_{0.32}$) at 0.2 g/mL polymer concentration and [ketone]:[alkoxyamine] = 1:1 within 2 h. When only 5 equiv of the monofunctional alkoxyamine was employed, 24 h was required for the gel-to-sol transition at 25 °C (Fig. 6). Similarly, the gel-to-sol transition became slower as the DAA content in the parent copolymer increased. The hydrogel prepared with P(DMA$_{0.6}$–*stat*–DAA$_{0.4}$) required 24 h to become a solution with 20 equiv of monofunctional alkoxyamine, and the hydrogel prepared with P(DMA$_{0.52}$–*stat*–DAA$_{0.48}$) never turned into a solution after several weeks at 25 °C, even with 50 equiv of monofunctional alkoxyamine. This observation is likely due to the relative hydrophobicity or the significantly reduced pore sizes within the highly-crosslinked hydrogels prepared with P(DMA$_{0.52}$–*stat*–DAA$_{0.48}$), which limited diffusion of the monofunctional alkoxyamine through the collapsed hydrogel matrix to retard the gel-to-sol transition.

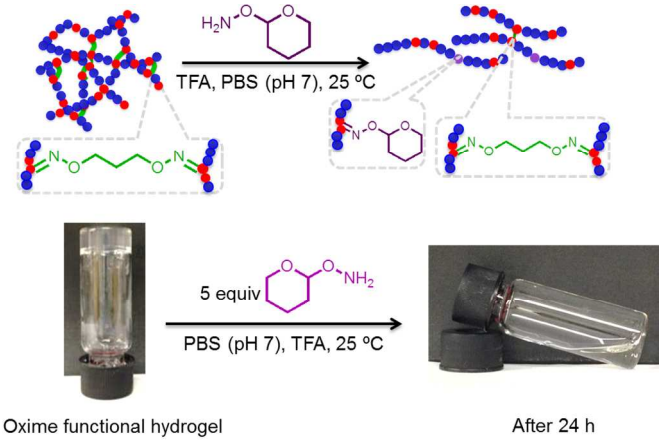

Fig. 6 Gel-to-sol transition of oxime-containing hydrogel prepared at [P(DMA$_{0.68}$–*stat*–DAA$_{0.32}$)] = 0.2 g/mL and [ketone]:[alkoxyamine] = 1:1. Addition of the monofunctional alkoxyamine led to crosslink cleavage via transoximination.

Self-healing behavior. While considerably more stable than imines, many oximes remain susceptible to cleavage under specific reaction conditions (*e.g.,* in presence of excess aldehyde/ketone and/or acid catalyst).[46] Moreover, hydrolytic cleavage of the oxime bond is reversible, which suggests that under carefully tuned aqueous conditions, the direction of the equilibrium between oximes and their alkoxyamine and ketone/aldehyde components can be tuned to permit facile oxime exchange.[34] We reasoned that reversible covalent bonds of this type could be used to induce self-healing behavior.[47]

To qualitatively assess the potential for self-healing, two round hydrogel samples were prepared with P(DMA$_{0.68}$–*stat*–DAA$_{0.32}$) and one equivalent of the difunctional alkoxyamine crosslinker. Each hydrogel sample was cut into two equal pieces. One half of each respective hydrogel was brought in contact with the other and allowed to remain in contact in a Petri dish containing sufficient moisture to avoid dehydration. We anticipated the intimate contact of the two hydrogel pieces would promote oxime exchange across the damage interface to effect covalent healing.[30,47] Healing occurred within 2 h, as evidenced by the gel qualitatively regaining its original mechanical strength, being capable of withstanding stretching with a tensile force applied perpendicular to the cut line. The gels were also capable of supporting their own weight when suspended under gravity for extended periods of time (Fig. 7). A similar process was repeated three additional times with the same piece of previously healed hydrogel. Successful healing was observed after every cycle. This behavior suggested healing occurs by oxime bond formation across the cut interface as the chemical functionalities gradually diffuse across the interface of the cut pieces.[46] The self-healing experiment was also performed with a hydrogel sample prepared with a different polymer concentration [P(DMA$_{0.68}$–*stat*–DAA$_{0.32}$)] = 0.05 g/mL) and stoichiometry ([ketone]:[alkoxyamine] = 1.5:1). Healing was observed after the cut pieces were brought together and kept in intimate contact for 2 h, suggesting that self-healing can be achieved with a variety of hydrogel compositions. Interestingly, hydrogels prepared with P(DMA$_{0.6}$–*stat*–DAA$_{0.4}$) and P(DMA$_{0.52}$–*stat*–DAA$_{0.48}$) did not heal under similar conditions even after being kept in contact for several days. The densely crosslinked network in those hydrogels may have hindered the diffusion of chains required to bridge the damage interface and bring about healing.

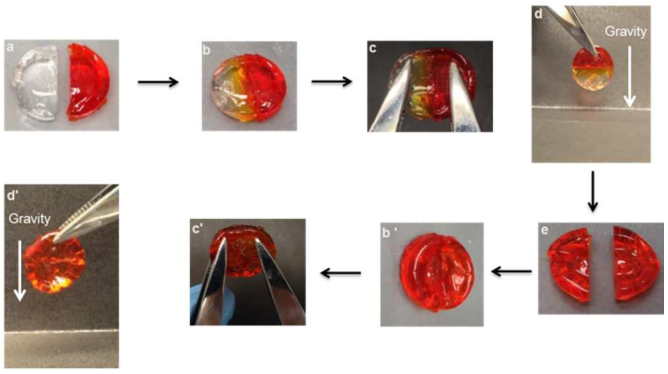

Fig. 7 Room temperature healing test of hydrogels prepared with P(DMA$_{0.68}$–*stat*–DAA$_{0.32}$) (0.2 g/mL) and [ketone]:[alkoxyamine] = 1:1. a) Two previously cut pieces of distinct hydrogel samples (a dye was added to one gel for clarity). b) and b′) The gel halves were placed in contact for 2 h. c) and c′) After healing for 2 h, the repaired gels were stretched with tweezers with tensile force being applied perpendicularly to the original cut. d) and d′) Healed gels suspended under gravity. e) After maturing the healed hydrogel for 24 h, the hydrogel was cut again along the previous cut line.

To obtain quantitative insight into the dynamic or reversible nature of oxime exchange, a hydrogel sample was prepared on the rheometer plate and matured for 2 h before being intentionally damaged during a strain sweep experiment (0.1-1000% strain), such that the elastic modulus became less than the viscous modulus upon strain-induced failure (Fig. 6). After reducing the strain to 50%, the crosslinks rapidly recoupled in less than 17 s to restore conditions under which G′>G″, suggesting the gels had regained much of their original structure. However, the moduli did not completely recover to their original values, which may indicate that the strain-induced failure also led to some irreversible carbon-carbon bond scission and/or partial loss of the sample during the strain sweep. Similar behavior was observed for the hydrogel prepared with 0.05 g/mL polymer concentration and [ketone]:[alkoxyamine] = 1.5:1 (Fig. S5).

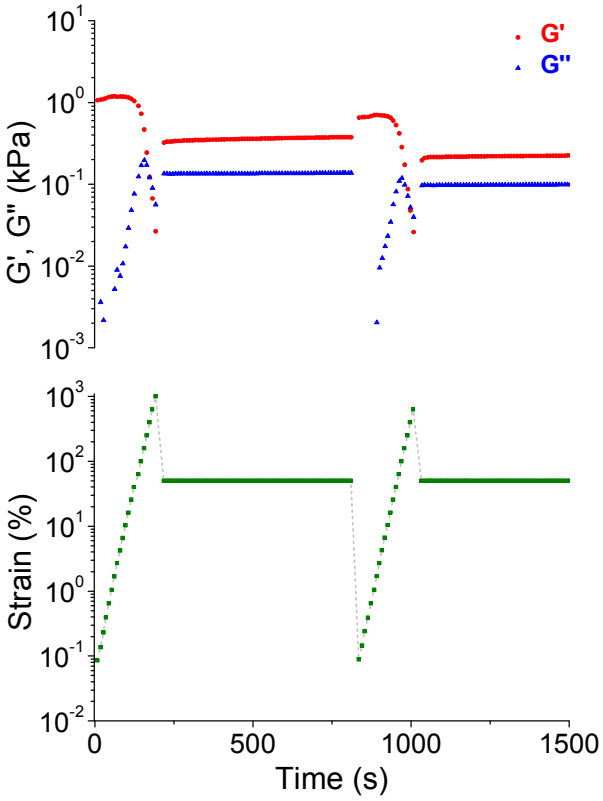

Fig. 8 Self-healing of hydrogels after fracture. The top plot shows the change in modulus (red and blue) during the strain ramp (green) described by the bottom plot. The hydrogel fractured during the strain ramp up to 387% and rapidly healed after the strain was reduced. The strain ramp was conducted at constant angular frequency of 10 rad/s and a constant temperature 25 °C using a 25 mm CP geometry. [P(DMA$_{0.68}$-*stat*-DAA$_{0.32}$)] = 0.2 g/mL, and [ketone]:[alkoxyamine] = 1:1

CONCLUSIONS

We demonstrated that ketoxime formation is an efficient route to prepare hydrogels that were both self-healing and stimuli-responsive. Several factors such as polymer composition, polymer concentration, stoichiometry, and temperature can be tuned to control the hydrogel properties. A significant rate of crosslinking was observed as the

polymer concentration and DAA content in the polymer was increased, whereas the stoichiometry of the crosslinker seemed to have minimal effect on the gelation kinetics. The reversible nature of oxime linkages led to reversible gel-to-sol transitions of the hydrogels in the presence of excess monofunctional alkoxyamine at ambient temperature and promoted autonomous healing in damaged hydrogel samples. Additionally, we observed that higher incorporation of crosslinks resulted in a stronger hydrogels but restricted the polymer chain mobility necessary to cause healing in a damaged hydrogel. We believe that the tunable degradation and healing behavior of these oxime hydrogels may offer a viable mean to design biosensors, shape-memory materials, and delivery vehicles for dyes and drugs.

Acknowledgements

This material is based upon work supported by the National Science Foundation (DMR-1410223). Acknowledgment is made to the Donors of the American Chemical Society Petroleum Research Fund (53225-ND7) for partial support of this research.

Notes and references

[a]George & Josephine Butler Polymer Research Laboratory, Center for Macromolecular Science & Engineering, Department of Chemistry, University of Florida, Gainesville, FL 32611-7200, USA
E-Mail: sumerlin@chem.ufl.edu

Electronic Supplementary Information (ESI) available: ^{1}H NMR, UV-VIS spectra, rheology results, and swelling ratios. See DOI: 10.1039/b000000x/

1. H. Colquhoun and B. Klumperman, *Polym. Chem.*, 2013, **4**, 4832-4833.
2. J. A. Syrett, C. R. Becer and D. M. Haddleton, *Polym. Chem.*, 2010, **1**, 978-987; J. Song, C. M. Thurber, S. Kobayashi, A. M. Baker, C. W. Macosko and H. C. Silvis, *Polymer*, 2012, **53**, 3636-3641; J. Song, A. Batra, J. M. Rego and C. W. Macosko, *Prog. Org. Coat.*, 2011, **72**, 492-497.
3. P. Fratzl, *J. R. Soc. Interface*, 2007, **4**, 637-642; V. Amendola and M. Meneghetti, *Nanoscale*, 2009, **1**, 74-88; M. W. Urban, *Nat. Chem.*, 2012, **4**, 80-82; B. Ghosh and M. W. Urban, *Science*, 2009, **323**, 1458-1460.
4. Y. Fang, C.-F. Wang, Z.-H. Zhang, H. Shao and S. Chen, *Sci. Rep.*, 2013, **3**, 1-7; P. Theato, B. S. Sumerlin, R. K. O'Reilly and I. I. I. T. H. Epps, *Chem. Soc. Rev.*, 2013, **42**, 7055-7056.
5. G. E. Fantner, E. Oroudjev, G. Schitter, L. S. Golde, P. Thurner, M. M. Finch, P. Turner, T. Gutsmann, D. E. Morse, H. Hansma and P. K. Hansma, *Biophys. J.*, 2006, **90**, 1411-1418.
6. G. Deng, F. Li, H. Yu, F. Liu, C. Liu, W. Sun, H. Jiang and Y. Chen, *ACS Macro Lett.*, 2012, **1**, 275-279.
7. R. J. Sheridan and C. N. Bowman, *Polym. Chem.*, 2013, **4**, 4974-4979; M. Pepels, I. Filot, B. Klumperman and H. Goossens, *Polym. Chem.*, 2013, **4**, 4955-4965; D. N. Amato, G. A. Strange, J. P. Swanson, A. D. Chavez, S. E. Roy, K. L. Varney, C. A. Machado, D. V. Amato and P. J. Costanzo, *Polym. Chem.*, 2014, **5**, 69-76.
8. S. Bode, R. K. Bose, S. Matthes, M. Ehrhardt, A. Seifert, F. H. Schacher, R. M. Paulus, S. Stumpf, B. Sandmann, J. Vitz, A. Winter, S. Hoeppener, S. J. Garcia, S. Spange, S. van der Zwaag, M. D. Hager and U. S. Schubert, *Polym. Chem.*, 2013, **4**, 4966-4973; M. Burnworth, L. Tang, J. R. Kumpfer, A. J. Duncan, F. L. Beyer, G. L. Fiore, S. J. Rowan and C. Weder, *Nature*, 2011, **472**, 334-337; S. J. Kalista and T. C. Ward, *J. R. Soc. Interface*, 2007, **4**, 405-411; S. Burattini, H. M. Colquhoun, J. D. Fox, D. Friedmann, B. W. Greenland, P. J. F. Harris, W. Hayes, M. E. Mackay and S. J. Rowan, *Chem. Commun.*, 2009, 6717-6719.
9. A. Phadke, C. Zhang, B. Arman, C.-C. Hsu, R. A. Mashelkar, A. K. Lele, M. J. Tauber, G. Arya and S. Varghese, *PNAS*, 2012, **109**, 4383-4388.
10. R. J. Wojtecki, M. A. Meador and S. J. Rowan, *Nat. Mater.*, 2011, **10**, 14-27; B. Karagoz, L. Esser, H. T. Duong, J. S. Basuki, C. Boyer and T. P. Davis, *Polym. Chem.*, 2014, **5**, 350-355; Y. Xu, Y. Li, X. Cao, Q. Chen and Z. An, *Polym. Chem.*, 2014, **5**, 6244-6255.
11. Q. Wang, J. L. Mynar, M. Yoshida, E. Lee, M. Lee, K. Okuro, K. Kinbara and T. Aida, *Nature*, 2010, **463**, 339-343; M. Yoshida, N. Koumura, Y. Misawa, N. Tamaoki, H. Matsumoto, H. Kawanami, S. Kazaoui and N. Minami, *J. Am. Chem. Soc.*, 2007, **129**, 11039-11041; D. C. Tuncaboylu, M. Sari, W. Oppermann and O. Okay, *Macromolecules*, 2011, **44**, 4997-5005.
12. G. Deng, C. Tang, F. Li, H. Jiang and Y. Chen, *Macromolecules*, 2010, **43**, 1191-1194.
13. Y. Zhang, L. Tao, S. Li and Y. Wei, *Biomacromolecules*, 2011, **12**, 2894-2901.
14. M. Nakahata, Y. Takashima, H. Yamaguchi and A. Harada, *Nat. Commun.*, 2011, **2**, 511.
15. J. A. Burdick and W. L. Murphy, *Nat. Commun.*, 2012, **3**, 1269.
16. P. M. Kharkar, K. L. Kiick and A. M. Kloxin, *Chem. Soc. Rev.*, 2013, **42**, 7335-7372.
17. S. Sahoo, C. Chung, S. Khetan and J. A. Burdick, *Biomacromolecules*, 2008, **9**, 1088-1092; S. J. Bryant and K. S. Anseth, *J. Biomed. Mater. Res. Part A*, 2003, **64A**, 70-79; W. Zhao, X. Jin, Y. Cong, Y. Liu and J. Fu, *J. Chem. Technol. Biotechnol.*, 2013, **88**, 327-339.
18. L. Dong, A. K. Agarwal, D. J. Beebe and H. Jiang, *Nature*, 2006, **442**, 551-554.
19. I. Tomatsu, A. Hashidzume and A. Harada, *Macromolecules*, 2005, **38**, 5223-5227; S. Tamesue, Y. Takashima, H. Yamaguchi, S. Shinkai and A. Harada, *Angew. Chem. Int. Ed.*, 2010, **49**, 7461-7464.
20. K. Sawahata, M. Hara, H. Yasunaga and Y. Osada, *J. Controlled Release*, 1990, **14**, 253-262.
21. S.-T. Fei, M. V. B. Phelps, Y. Wang, E. Barrett, F. Gandhi and H. R. Allcock, *Soft Matter*, 2006, **2**, 397-401.
22. T. Yang, R. Ji, X.-X. Deng, F.-S. Du and Z.-C. Li, *Soft Matter*, 2014, **10**, 2671-2678.
23. C. Tsitsilianis, *Soft Matter*, 2010, **6**, 2372-2388.
24. F. Liu, F. Li, G. Deng, Y. Chen, B. Zhang, J. Zhang and C.-Y. Liu, *Macromolecules*, 2012, **45**, 1636-1645.
25. D. D. McKinnon, D. W. Domaille, J. N. Cha and K. S. Anseth, *Chem. Mater.*, 2014, **26**, 2382-2387.
26. D. E. Whitaker, C. S. Mahon and D. A. Fulton, *Angew. Chem. Int. Ed.*, 2013, **52**, 956-959.

27. K. C. Koehler, K. S. Anseth and C. N. Bowman, *Biomacromolecules*, 2013, **14**, 538-547; S. Kirchhof, F. P. Brandl, N. Hammer and A. M. Goepferich, *J. Mater. Chem. B*, 2013, **1**, 4855-4864.
28. S.-Y. Choh, D. Cross and C. Wang, *Biomacromolecules*, 2011, **12**, 1126-1136; C. Yang, D. Li, Q. FengZhao, L. Wang, L. Wang and Z. Yang, *Org. Biomol. Chem.*, 2013, **11**, 6946-6951; H. A. Aliyar, P. D. Hamilton and N. Ravi, *Biomacromolecules*, 2004, **6**, 204-211; A. P. Vogt and B. S. Sumerlin, *Soft Matter*, 2009, **5**, 2347-2351.
29. L. He, D. E. Fullenkamp, J. G. Rivera and P. B. Messersmith, *Chem. Commun.*, 2011, **47**, 7497-7499.
30. C. C. Deng, W. L. A. Brooks, K. A. Abboud and B. S. Sumerlin, *ACS Macro Lett.*, 2015, **4**, 220-224.
31. J. Su, Y. Amamoto, M. Nishihara, A. Takahara and H. Otsuka, *Polym. Chem.*, 2011, **2**, 2021-2026.
32. A. P. Esser-Kahn and M. B. Francis, *Angew. Chem. Int. Ed.*, 2008, **47**, 3751-3754; C. E. Schmidt, H. John G. and L. Phillip, *J. Biomater. Sci., Polym. Ed.*, 2015, **26**, 143-161; M. R. Hill, S. Mukherjee, P. J. Costanzo and B. S. Sumerlin, *Polym. Chem.*, 2012, **3**, 1758-1762.
33. A. P. Esser-Kahn, V. Trang and M. B. Francis, *J. Am. Chem. Soc.*, 2010, **132**, 13264-13269.
34. V. A. Polyakov, M. I. Nelen, N. Nazarpack-Kandlousy, A. D. Ryabov and A. V. Eliseev, *J. Phys. Org. Chem.*, 1999, **12**, 357-363.
35. G. N. Grover, J. Lam, T. H. Nguyen, T. Segura and H. D. Maynard, *Biomacromolecules*, 2012, **13**, 3013-3017.
36. F. Lin, J. Yu, W. Tang, J. Zheng, A. Defante, K. Guo, C. Wesdemiotis and M. L. Becker, *Biomacromolecules*, 2013, **14**, 3749-3758.
37. A. Pulsipher, D. Dutta, W. Luo and M. N. Yousaf, *Angew. Chem. Int. Ed.*, 2014, **53**, 9487-9492; S. Park, N. P. Westcott, W. Luo, D. Dutta and M. N. Yousaf, *Bioconjugate Chem.*, 2014, **25**, 543-551; M. Axelson, *Anal. Biochem.*, 1978, **86**, 133-141.
38. S. Mukherjee, A. P. Bapat, M. R. Hill and B. S. Sumerlin, *Polym. Chem.*, 2014, **5**, 6923-6931.
39. A. P. Bapat, J. G. Ray, D. A. Savin, E. A. Hoff, D. L. Patton and B. S. Sumerlin, *Polym. Chem.*, 2012, **3**, 3112-3120; A. P. Bapat, J. G. Ray, D. A. Savin and B. S. Sumerlin, *Macromolecules*, 2013, **46**, 2188-2198; A. P. Bapat, D. Roy, J. G. Ray, D. A. Savin and B. S. Sumerlin, *J. Am. Chem. Soc.*, 2011, **133**, 19832-19838.
40. J.-M. Lehn, *Chem. Eur. J.*, 1999, **5**, 2455-2463.
41. X. Tang, J. Han, Z. Zhu, X. Lu, H. Chen and Y. Cai, *Polym. Chem.*, 2014, **5**, 4115-4123.
42. D. Roy, W. L. A. Brooks and B. S. Sumerlin, *Chem. Soc. Rev.*, 2013, **42**, 7214-7243; P. De and B. S. Sumerlin, *Macromol. Chem. Phys.*, 2013, **214**, 272-279.
43. M. Philipp, U. Muller, R. J. Jimenez Rioboo, R. Sanctuary, P. Muller-Buschbaum and J. K. Kruger, *Soft Matter*, 2013, **9**, 9887-9896; H. G. Schild, M. Muthukumar and D. A. Tirrell, *Macromolecules*, 1991, **24**, 948-952.
44. J. Liu, R. C. Li, G. J. Sand, V. Bulmus, T. P. Davis and H. D. Maynard, *Macromolecules*, 2012, **46**, 8-14; K. L. Heredia, Z. P. Tolstyka and H. D. Maynard, *Macromolecules*, 2007, **40**, 4772-4779.
45. G. N. Grover, R. L. Braden and K. L. Christman, *Adv. Mater.*, 2013, **25**, 2937-2942.
46. J. Kalia and R. T. Raines, *Angew. Chem. Int. Ed.*, 2008, **47**, 7523-7526.
47. Z. Wei, J. H. Yang, J. Zhou, F. Xu, M. Zrinyi, P. H. Dussault, Y. Osada and Y. M. Chen, *Chem. Soc. Rev.*, 2014, **43**, 8114-8131.